LANGMUIR

Article

pubs.acs.org/Langmuir

Conserved Molecular Superlattices in a Series of Homologous Synthetic Mycobacterial Cell-Wall Lipids Forming Interdigitated Bilayers

Birte Martin-Bertelsen,[*,†] Anan Yaghmur,[†] Henrik Franzyk,[‡] Sarah Justesen,[†,‡] Jacob J. K. Kirkensgaard,[*,§,∥] and Camilla Foged[*,†,∥]

[†]Department of Pharmacy and [‡]Department of Drug Design and Pharmacology, Faculty of Health and Medical Sciences, University of Copenhagen, Universitetsparken 2, DK-2100 Copenhagen, Denmark

[§]Niels Bohr Institute, Faculty of Science, University of Copenhagen, Universitetsparken 5, 2100 Copenhagen, Denmark

Supporting Information

ABSTRACT: Synthetic analogues of the cell-wall lipid monomycoloyl glycerol (MMG) are promising as next-generation vaccine adjuvants. In the present study, the thermotropic phase behavior of an array of synthetic MMG analogues was examined by using simultaneous small- and wide-angle X-ray scattering under excess water conditions. The MMG analogues differed in the alkyl chain lengths and in the stereochemistry of the polar glycerol headgroup or of the lipid tails (native-like versus alternative compounds). All MMG analogues formed poorly hydrated lamellar phases at low temperatures and inverse hexagonal (H_2) phases at higher temperatures prior to melting. MMG analogues with a native-like lipid acid configuration self-assembled into noninterdigitated bilayers whereas the analogues displaying an alternative lipid acid configuration formed interdigitated bilayers in a subgel ($L_{c'}$) state. This is in contrast to previously described interdigitated phases for other lipids, which are usually in a gel (L_β) state. All investigated MMG analogues displayed an abrupt direct temperature-induced phase transition from $L_{c'}$ to H_2. This transition is ultimately driven by the lipid chain melting and the accompanying change in molecular shape. No intermediate structures were found, but the entire array of MMG analogues displayed phase coexistence during the lamellar to H_2 transition. The structural data also showed that the headgroups of the MMG analogues adopting the alternative lipid acid configuration were ordered and formed a two-dimensional molecular superlattice, which was conserved regardless of the lipid tail length. To our knowledge, the MMG analogues with an alternative lipid acid configuration represent the first example of a lipid system showing both interdigitation and superlattice formation, and as such could serve as an interesting model system for future studies. The MMG analogues are also relevant from a subunit vaccine perspective because they are well-tolerated and display promising immunopotentiating activity. The structural characterization described here will serve as a prerequisite for the rational design of nanoparticulate adjuvants with specific and tailored structural features.

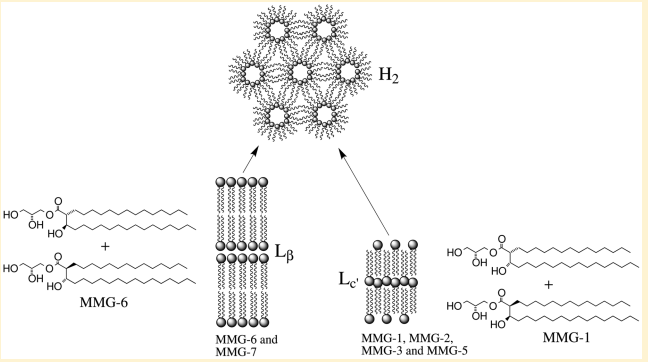

INTRODUCTION

A number of mycobacterial cell-wall components are recognized to possess potent immunostimulatory activity.[1,2] A vaccination strategy utilizing these cell-wall components as adjuvants in subunit vaccines, in combination with highly purified or synthetic pathogen-specific antigen(s), therefore appears to be a promising prophylactic approach for the prevention of certain infectious diseases.[3,4] The apolar lipid monomycoloyl glycerol (MMG) has been identified as one of the most potent immunostimulatory membrane lipids from the cell wall of *Mycobacterium bovis* Bacillus Calmette-Gúerin (*M. bovis* BCG).[5] A synthetic MMG analogue, referred to as MMG-1, has been shown to both be well-tolerated and possess immunostimulatory properties comparable to the immunostimulatory properties of the natural MMG.[5] MMG-1 is composed of a hydrophilic glycerol headgroup linked via an ester bond to a hydrophobic acid displaying saturated C_{14}/C_{15} lipid tails (Figure 1).[6] Furthermore, a dispersion based on MMG-1 and the quaternary ammonium salt dimethyldioctadecylammonium (DDA) bromide has been engineered into a promising liposome-based cationic adjuvant (termed CAF04, Statens Serum Institut, Denmark) that induces attractive cell-mediated immune (CMI) responses in addition to antibody-mediated immune responses.[6] The majority of adjuvants used in licensed vaccines nowadays only induce an antibody-mediated immune response, although induction of a CMI

Received: May 6, 2016
Revised: October 12, 2016
Published: November 7, 2016

DOI: 10.1021/acs.langmuir.6b01720
Langmuir XXXX, XXX, XXX−XXX

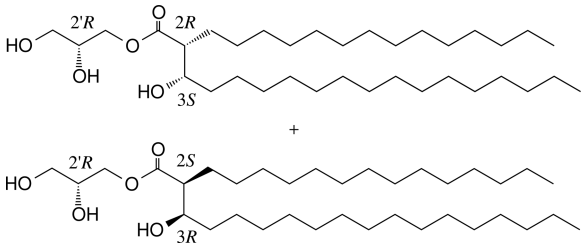

Figure 1. Molecular structure of the synthetic MMG analogues exemplified by MMG-1, which consists of a 1:1 mixture of two diastereomers with a (2*R*,3*S*) and a (2*S*,3*R*) lipid configuration, respectively. The alkyl chain length for MMG-1 is C_{14}/C_{15}, and the configuration of the glycerol headgroup is 2′*R*.

response is a prerequisite for successful vaccination against intracellular pathogens, e.g. HIV, *M. tuberculosis*, and *Chlamydia trachomatis*.[7,8]

Based on MMG-1, an array of analogues was designed by systematic variation of the length of the hydrophobic alkyl chains and the stereochemistry of both the hydrophilic headgroup and the lipid acid moiety.[9,10] We classified the lipids into two groups depending on the stereochemistry, displaying either a "native-like" (N) or an "alternative" (A) racemic corynomycolic acid configuration (Table 1). Previously, we have studied the self-assembled nanostructures of these MMG analogues in excess water or serum-containing cell medium at physiologically relevant temperatures (25, 35, and 40 °C).[9,10] These studies demonstrated that the length of the alkyl chains and the stereochemistry of the lipid acid moiety have a pronounced impact on the self-assembled nanostructures of the MMG analogues in excess water. The MMG analogues display either a lamellar or an inverse hexagonal structure at 25, 35, and 40 °C.[9,10] The immunostimulatory activity of these compounds was also tested *in vitro*, and a correlation between the supramolecular structure of the MMG analogues and their ability to stimulate human monocyte-derived dendritic cells was established, indicating that the analogues adopting an inverse hexagonal structure were less capable of stimulating the dendritic cells as compared to the analogues adopting a lamellar structure.[9] Incorporation of the MMG analogues into DDA vesicles resulted in the formation of unilamellar vesicles, multilamellar vesicles or particles with an internal inverse hexagonal (H_2) structure, depending on the specific MMG analogue and the molar ratio of MMG to DDA.[10] Selected binary dispersions based on DDA in combination with MMG-1, MMG-3, or MMG-6 (Table 1) were furthermore shown to be immunoactive in mice and induced strong Th1 and Th17 responses.[10]

Table 1. Overview of the Designed MMG Analogues[a]

name	headgroup stereochemistry	stereochemistry of lipid acid moiety	chain lengths
MMG-1 (A)	2′*R*	(2*R*,3*S*)/(2*S*,3*R*)	C_{14}/C_{15}
MMG-2 (A)	2′*R*	(2*R*,3*S*)/(2*S*,3*R*)	C_{16}/C_{17}
MMG-3 (A)	2′*R*	(2*R*,3*S*)/(2*S*,3*R*)	C_{10}/C_{11}
MMG-4 (A)[b]	2′*R*	(2*R*,3*S*)/(2*S*,3*R*)	C_6/C_7
MMG-5 (A)	2′*S*	(2*R*,3*S*)/(2*S*,3*R*)	C_{14}/C_{15}
MMG-6 (N)	2′*R*	(2*R*,3*R*)/(2*S*,3*S*)	C_{14}/C_{15}
MMG-7 (N)	2′*S*	(2*R*,3*R*)/(2*S*,3*S*)	C_{14}/C_{15}

A: Alternative racemic corynomycolic acid configuration. N: Native-like racemic corynomycolic acid configuration. [a]Table adapted from Martin-Bertelsen & Korsholm et al.[9] with permission from the Royal Society of Chemistry. [b]Not included in this study.

Despite these efforts, a systematic study of the phase behavior of the different synthetic MMG analogues in excess water has not yet been performed. The influence of the molecular properties on the self-assembling properties in excess water of both natural and synthetic lipids is well-studied in the literature,[11−14] but remains to be fully understood for the MMG analogues. In the present study, the effect on the self-assembled nanostructure due to alterations in the tail length and in the stereochemistry of both the hydrophilic headgroup and the lipid acid moiety was extensively studied in excess buffer as a function of temperature by using simultaneous small- and wide-angle X-ray scattering (SAXS and WAXS, respectively). Thus, the dependence on temperature for the packing of the lipid alkyl chains and the organization of the lipid molecules into supramolecular structures was established for the array of MMG analogues.

MATERIALS AND METHODS

Materials. The used chemicals and reagents were obtained commercially at analytical grade.

Synthesis of MMG Analogues. An array of MMG analogues varying in the stereochemistry and lipid chain lengths (Table 1) were synthesized and purified as previously described, and the identity and purity of the resulting compounds were confirmed by NMR spectroscopy.[6,9] The MMG-4 analogue was not included in the present study because the compound is oil-like at ambient temperature and thus clearly not forming neither a crystalline nor a liquid crystalline phase in excess buffer.

Sample Preparation for SAXS/WAXS. *Hydrated Samples.* The dry lipid powders were hydrated by adding Tris buffer (10 mM, pH 7.4) and carrying out at least five freeze−thaw cycles between liquid nitrogen/dry ice and room temperature, and then homogenizing several times during the thawing steps by vigorous vortexing and heating above the crystalline-to-liquid crystalline phase transition temperature. The final lipid concentration was 100 mg/mL, and the samples were incubated at room temperature for at least 1 week before performing the SAXS/WAXS measurements to ensure optimal hydration of the samples.

Anhydrous Sample (MMG-1). MMG-1 was dissolved in dichloromethane, and the organic solvent was evaporated repeatedly, and then the sample was dried further under vacuum (freeze-dryer) for 2 days. NMR spectroscopy measurements confirmed that no H_2O was bound.[9] The sample was stored at −20 °C.

SAXS/WAXS Measurements and Data Analysis. The X-ray measurements were performed by using a SAXSLab instrument (JJXray, Kgs. Lyngby, DK) equipped with a 100XL + microfocus sealed X-ray tube (Rigaku, Tokyo, JP) producing a photon beam with a wavelength of 1.54 Å. The scattering patterns were recorded with a two-dimensional (2D) 300 K Pilatus pixel area detector (Dectris, Baden, CH). The samples were measured in a temperature-controllable sample stage (Linkam, Tadworth, UK). The heating rate was 10 °C/min, and the investigated temperature range was 25−80 °C (15−80 °C for MMG-6). The samples were left for 10 min to equilibrate before measuring at each temperature step. The 2D scattering data did not show any angular dependency and were thus azimuthally averaged, normalized by the incident radiation intensity, the sample exposure time and transmission, and corrected for background and detector inhomogeneities. The radially averaged intensity I is given as a function of the scattering vector $q = 4\pi \sin \theta/\lambda$, where λ is the wavelength and 2θ is the scattering angle. The samples were measured at two settings: A setting covering a q-range from approximately 0.004 to 0.9 $Å^{-1}$ with a sample exposure time of 600 s, and a setting covering a q-range from approximately 0.02 to 3 $Å^{-1}$ with an exposure time of 300 s. Silver behenate [$H_3C(CH_2)_{20}COOAg$] with a d-spacing value of 58.38 Å was used as a standard to calibrate

DOI: 10.1021/acs.langmuir.6b01720
Langmuir XXXX, XXX, XXX−XXX

the angular scale for the small-angle setting.[15] A silicon powder with a NIST (National Institute of Standards and Technology) certified lattice parameter of 5.43 Å was used to calibrate the wide-angle region (Standard Reference Material 640d). The mean lattice parameter (l) was calculated from the peak position (p) of the first order reflection according to the rules for the different mesophases.[16] The peak position and full width at half-maximum (fwhm) was estimated by fitting a Gaussian to the peak. A standard deviation (SD) was calculated from the fwhm value (fwhm $=2\sqrt{2\ln 2}$ SD) and propagated to the lattice parameter ($SD_l = l\ SD_p/p$). The scattering plots were prepared using MATLAB (The MathWorks, Inc., MA, USA). The fitting of the peaks was performed using the MATLAB script peakfit (O'Haver, Peak fitting program for time-series signals, version 5.7). The phase diagrams (Figures 3 and 9) were prepared using R (R Foundation for Statistical Computing, Vienna, AT). The chain−chain spacings for the MMG analogues were calculated from the reflections observed in the WAXS regime.[17] Electron density profiles were calculated from the measured intensities of the diffraction peaks following the procedure illustrated by Bottier et al.[18]

RESULTS AND DISCUSSION

MMG Analogues with an Alternative Lipid Acid Configuration Exhibit a Temperature-Induced Transition from a Crystalline Interdigitated Lamellar to an Inverse Hexagonal Phase. MMG analogues displaying different alkyl chain lengths, but with the alternative configuration of the lipid acid moieties (MMG-1, MMG-2, and MMG-3, respectively), exhibited similar thermotropic phase behavior in excess buffer at the studied temperatures. The X-ray scattering patterns revealed a direct transition from a lamellar to an inverse hexagonal (H_2) phase upon heating (Figure 2). A complete melting of the lipids was observed for MMG-1 and MMG-3 at higher temperatures with a likely formation of inverse-type micelles (M_2), albeit the characteristic scattering from micelles was not conclusively observed at the relatively short measuring times employed. The calculated d-spacings for the lamellar phase at 25 °C (dashed lines, Figure 2) were 24.2 Å for MMG-1, 26.8 Å for MMG-2, and 18.6 Å for MMG-3 (Table 2). As expected, the d-spacing was directly proportional to the alkyl chain length. Similarly, an increase in the phase transition temperature for increased alkyl chain lengths was evident (Figure 3). The unit parameters of the observed H_2 phases were calculated based on the scattering patterns recorded above the phase transitions (Table 2).

The measured bilayer spacings suggest that these MMG analogues adopt an interdigitated lamellar phase (Figure 4), as the observed lattice spacings are relatively small compared to the lattice spacings reported for other saturated lipids with comparable chain lengths,[19] and approximately half of the value of the bilayer spacing of the MMG analogues adopting a native lipid acid configuration (comparing MMG-1 with MMG-6 and MMG-7 which have identical chain lengths, cf. the discussion below). We do not consider a tilted chain arrangement likely because the WAXS pattern does not show the characteristic broad shoulder on the high q-side of the main peak,[20,21] and it would also require an extreme molecular tilt angle with respect to the bilayer normal to account for the observed bilayer spacings. The scattering patterns in the wide-angle region indicate that the lipid tails were well-ordered and suggest that the lipids were either in a gel or a crystalline state (Figure 2).

For all three MMG analogues with an alternative lipid acid configuration, an additional peak was observed between the first and the second reflection of the lamellar phase at approximately q = 0.4 $Å^{-1}$ with a corresponding Bragg spacing of approximately d = 16 Å (Figure 2, black asterisk). An evaluation of the peak position behavior as a function of temperature for these three MMG analogues revealed that this peak is associated with the packing in the lateral plane, *i.e.* the same plane as the hydrocarbon chains (Figure 5). The in-plane and out-of-plane correlations are clearly distinct in all three cases. We attribute this peak to the lateral packing of the lipid headgroups, where one of the headgroup-to-headgroup distances in the 2D plane corresponds well to approximately 16 Å, since the headgroup-to-headgroup distance is generally increased for the interdigitated bilayer (Figure 4). This is

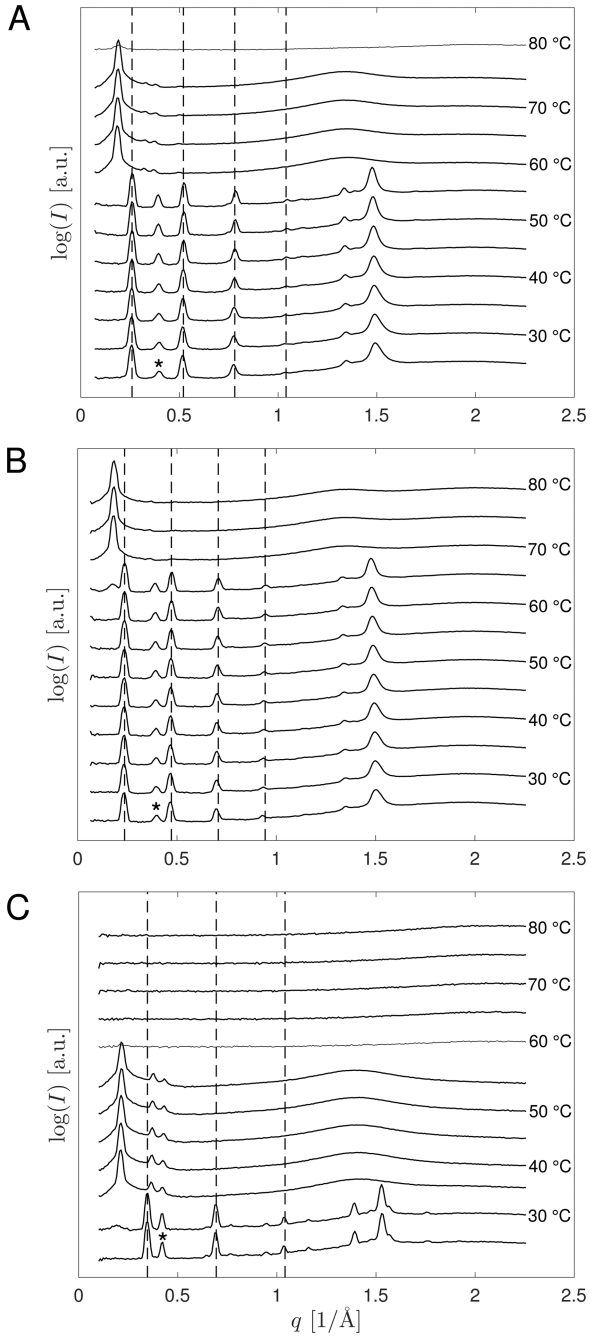

Figure 2. Scattering patterns of (A) MMG-1, (B) MMG-2, and (C) MMG-3 in excess buffer in steps of 5 °C in the temperature range of 25−80 °C. The dashed lines mark the detected reflections of the lamellar phases in the SAXS regime. The asterisks mark the reflections attributed to the lateral packing of the lipid headgroups.

DOI: 10.1021/acs.langmuir.6b01720
Langmuir XXXX, XXX, XXX−XXX

Table 2. Structural Parameters for the Self-Assemblies of the Investigated MMG Analogues in Excess Buffer[a]

compd	alkyl chains	lamellar d-spacing ± SD (Å)	H_2 unit cell parameter ± SD (Å)	lateral headgroup spacing ± SD (Å)	chain−chain spacing ± SD (Å)
MMG-1	C_{14}/C_{15}	24.2 ± 0.3	38.6 ± 0.4 (60 °C)	15.7 ± 0.4	4.86 ± 0.04
MMG-2	C_{16}/C_{17}	26.8 ± 0.3	39.8 ± 0.4 (70 °C)	15.7 ± 0.3	4.83 ± 0.04
MMG-3	C_{10}/C_{11}	18.6 ± 0.1	35.1 ± 0.3 (35 °C)	15.2 ± 0.1	4.74 ± 0.02
MMG-5	C_{14}/C_{15}	24.1 ± 0.5	38.5 ± 0.5 (60 °C)	15.6 ± 0.6	4.8 ± 0.1
MMG-6	C_{14}/C_{15}	51.4 ± 1.3 (15 °C)	40.4 ± 0.5		4.88 ± 0.05 (15 °C)
MMG-7	C_{14}/C_{15}	51.6 ± 1.3 (15 °C)	40.5 ± 1.6		4.9 ± 0.1 (15 °C)

[a]Calculations were performed for measurements at 25 °C if not otherwise indicated.

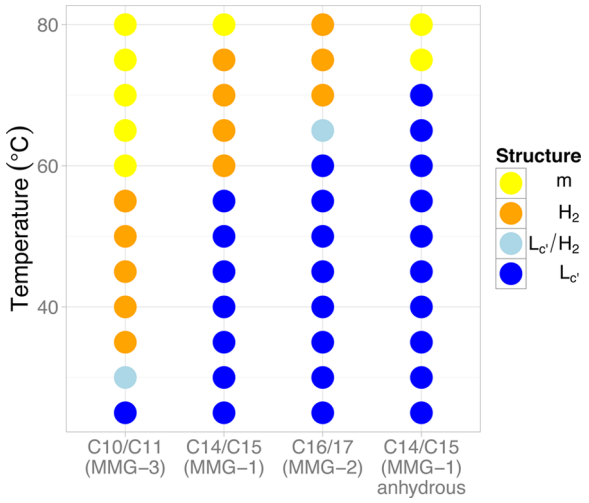

Figure 3. Dependency of the observed phases on the chain length of the MMG analogues with an alternative lipid acid configuration in excess buffer. The temperature range is 25−80 °C depicted in steps of 5 °C. Anhydrous MMG-1 is included for comparison. The observed structural phases are subgel ($L_{c'}$), inverse hexagonal (H_2), and a complete melting of the lipids (m).

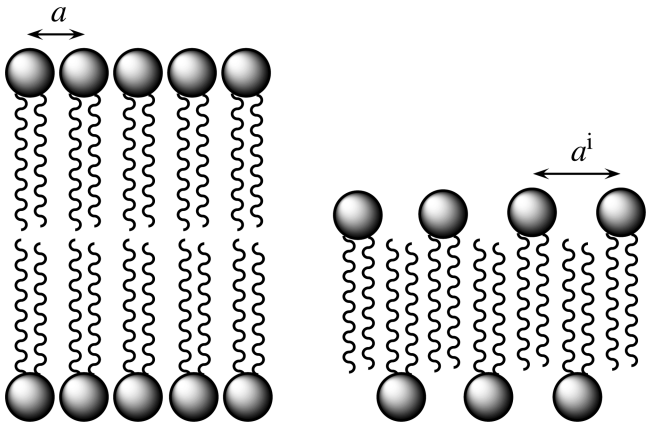

Figure 4. Schematic representation of noninterdigitated (left) and interdigitated (right) lipid membranes. The headgroup-to-headgroup distance is given by a for the noninterdigitated and a^i for the interdigitated lipid membrane.

further supported by the fact that the peak was conserved for the three analogues that all display the same headgroup stereochemistry. Thus, it is inferred that the lipid headgroups were in an ordered state, which means that the observed interdigitated lamellar phase was subgel ($L_{c'}$).[19]

In addition, a comparison at 25 °C of anhydrous MMG-1 and MMG-1 in excess buffer revealed that these two physical states have very similar structural characteristics (Figure 6).

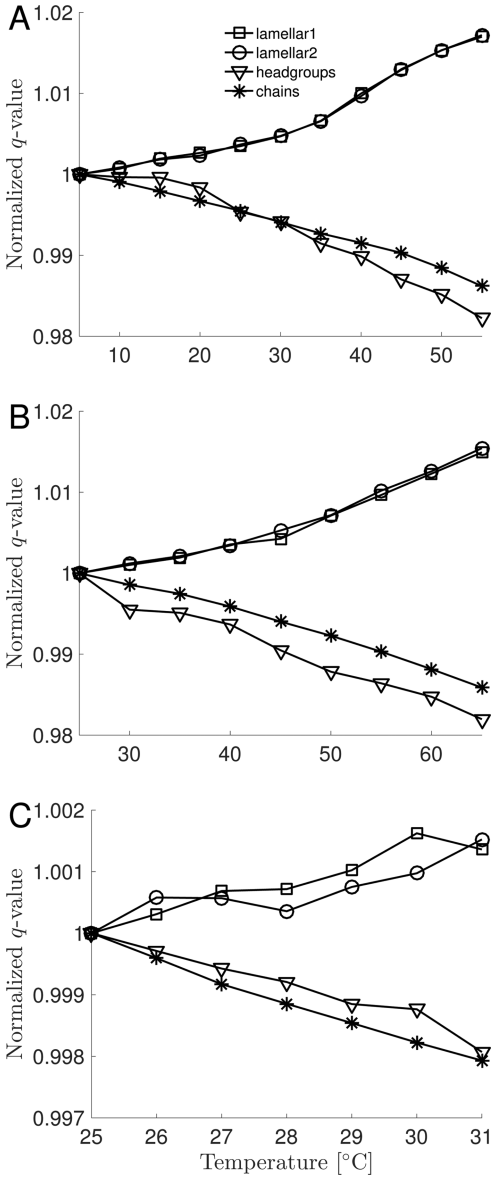

Figure 5. Peak position behavior as a function of temperature for (A) MMG-1, (B) MMG-2, and (C) MMG-3 normalized to the lowest temperature q-value. Square and circle markers correspond to the first two reflections of the lamellar phase, while asterisk markers correspond to the peak from the hydrocarbon chains, and triangle markers correspond to the headgroup peak at $q \approx 0.4$ Å^{-1}. Lines connecting the markers are inserted as a guide for the eye. The comparably small variation in the q-values for MMG-3 is due to the relatively small temperature range in which the headgroup peak was detected for this analogue.

DOI: 10.1021/acs.langmuir.6b01720
Langmuir XXXX, XXX, XXX−XXX

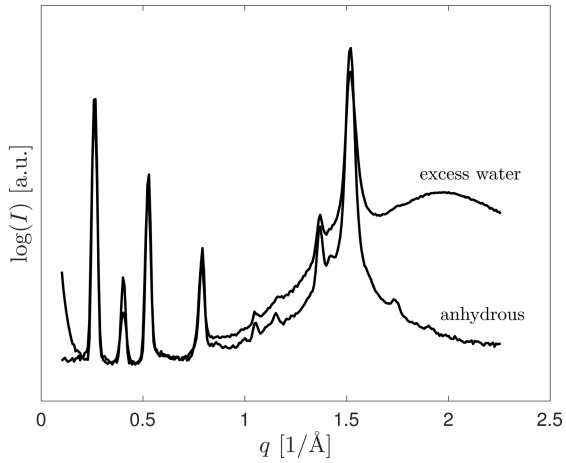

Figure 6. Comparison of the scattering patterns for the MMG-1 analogues in excess buffer and the anhydrous MMG-1 analogue at 25 °C.

This implies that the headgroup hydration of MMG-1 is generally poor and emphasizes that the resulting interdigitated lamellar phase observed for MMG-1 in excess buffer is crystalline. The lipid chain packing in the interdigitated gel phase (L_{β}^{i}) is commonly of the hexagonal type where each lipid chain has six nearest neighbors.[17] For the MMG analogues 1–3, we observed an interdigitated packing of the lipid chains with a dominant strong reflection at $q \approx 1.5$ Å^{-1}, which corresponds well to the characteristic single reflection for the hexagonal chain packing.[17] The calculated chain–chain spacings for the MMG analogues (Table 2) are based on the hexagonal chain packing where the chain–chain spacing is given by $a_{ch} = 2d/\sqrt{3}$.[17] The assignment of the additional weaker peaks in the WAXS region has not been unambigously resolved, but they are most likely attributed to additional diffractions from the headgroup organization in the $L_{c'}$ phase. Structures like these have previously been described by Katsaras et al. for the phospholipid dipalmitoylphosphatidylcholine (DPPC) in the crystalline/subgel $L_{c'}$ noninterdigitated phase.[22−25] Thus, our findings indicate that the interdigitated lamellar phase is in an $L_{c'}$ state, while previously reported interdigitated phases have mainly been observed in the gel (L_{β}) state.[19]

On heating, the sequence of thermotropic phase transitions in lipid membranes is usually: Lamellar crystalline L_c ↔ lamellar gel L_{β} ↔ lamellar liquid crystalline L_{α} ↔ bilayer cubic Q_2^B ↔ inverted hexagonal H_2 ↔ inverted micellar cubic Q_2^M ↔ micellar M_2.[26] Additional scattering data with a temperature resolution of 1 °C/step (Supporting Information, Figures S1–S2) revealed no intermediate stable structures at the measured resolution, and thus the transition from the crystalline lamellar phase ($L_{c'}$) to the inverse hexagonal phase appears to be direct. This observation was supported by a preliminary differential scanning calorimetry (DSC) study of MMG-1 in excess buffer, which revealed an endothermic phase transition with a transition temperature of approximately 59 °C assigned to the transition from the $L_{c'}$ to the H_2 phase on the basis of the X-ray diffraction observations (Supporting Information, Figure S4). The phase transition temperature is in agreement with the transition temperature suggested by the SAXS/WAXS data. A second phase transition observed at approximately 81 °C corresponds to the complete melting of the lipids, which was also observed by SAXS/WAXS.

A direct transition from a crystalline lamellar to an inverse hexagonal phase has been previously observed for long-chained glycolipids.[26] It has been reported that a direct transition from an L_c to an H_2 phase can be achieved by low-temperature annealing for a specific class of glycerols.[27,28] The direct transition from a crystalline lamellar to an inverse hexagonal phase, combined with the poor hydration properties of the MMG-1 analogue, suggest that the lipid–lipid interactions are very strong leading to the formation of rigid structures. In all samples the transition to the inverse hexagonal phase coincides with the melting of the lipid chains and is ultimately driven by this event. The melting of the chains induces a strong molecular shape transformation, leading to highly splayed chains favoring the immediate formation of the curved H_2 phase.

A comparison of the phase behavior as a function of temperature for both MMG-1 in excess buffer and anhydrous MMG-1 revealed that the complete melting temperature of both samples was comparable, although a slight decrease in the melting temperature was detected for the anhydrous sample as compared to the sample in excess buffer (Supporting Information, Figure S3). This reflects the dominance of the hydrophobic interactions in the crystalline phase, which have to be overcome for a complete transition to the fluid self-assembled H_2 nanostructure. Anhydrous MMG-1 did not exhibit a phase transition to an inverse hexagonal phase (Supporting Information, Figure S3). Interestingly, the interdigitated chain arrangement was conserved in the anhydrous state, which is not commonly observed. So far, the interdigitated phase has mainly been observed in the gel state for a range of phospholipids,[19] but a similar behavior was reported for ethyl-DPPC, where interdigitation is also observed in the anhydrous state.[29]

Comparison of the scattering patterns for both MMG-1 and MMG-5, which differ only in the headgroup stereochemistry, revealed no pronounced differences in the self-assembled structure (Figure 7). Expectedly, the phase behavior as a function of temperature was identical for the two analogues (which are mirror images, data not shown). This is in agreement with our recently reported observations at 35 and 40 °C, but in that report we characterized the lamellar phase of the MMG-1 and MMG-5 analogues as a liquid crystalline lamellar phase based solely on the SAXS experiments.[9] Based on the extended set of experiments performed in the present study (WAXS and the extended temperature range), we can now conclude that the lamellar phase mentioned above is not a liquid crystalline phase, but rather as a subgel phase, which exhibits a direct temperature-induced transition to an inverse hexagonal phase. Previously, a very weak peak observed at approximately 0.1 Å^{-1} was interpreted as the first reflection of the liquid crystalline lamellar phase, but this peak was not observed in the present study. Furthermore, this peak did not fit with the observed pattern of peaks associated with a lamellar phase, and it is now clear that this peak is not the first reflection of the lamellar phase. The observed difference seems to be attributed to a slight difference in the sample preparation technique, which in the previous study was based on a thin film rehydration method (cf. Supporting Information, Figure S5).[9]

The Configuration of the Lipid Acid Moiety of the MMG Analogues Has a Pronounced Influence on the Phase Behavior. Our previous study indicated that the lipid acid configuration has a pronounced impact on the self-assembled structure of MMG analogues investigated at 25, 35, and 40 °C, respectively.[9,10] The SAXS/WAXS data obtained in

DOI: 10.1021/acs.langmuir.6b01720
Langmuir XXXX, XXX, XXX−XXX

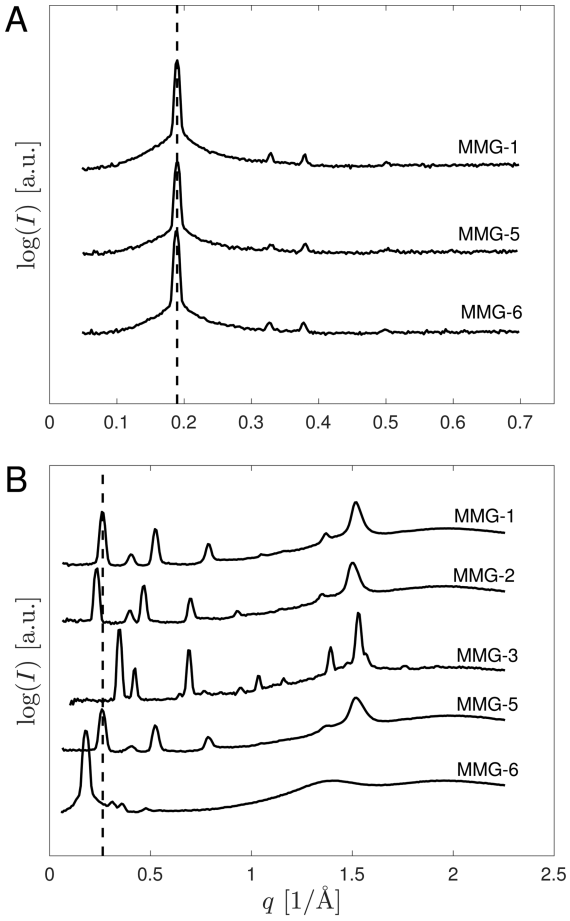

Figure 7. Comparison of the X-ray scattering patterns for selected MMG analogues. (*A*) MMG-1, MMG-5, and MMG-6 in excess buffer at 75 °C. All three analogues display an H_2 phase with identical lattice parameters. The first reflection of the H_2 phase is marked by a dashed black line. (B) MMG-1, MMG-2, MMG-3, MMG-5, and MMG-6 in excess buffer at 25 °C. MMG-1, MMG-2, MMG-3 and MMG-5 display an interdigitated $L_{c'}$ phase, while MMG-6 displays a liquid crystalline H_2 phase. The first reflection of the lamellar phase for MMG-1 is marked by a dashed black line.

the present study confirm this observation, as both the phase transition temperature from a lamellar to an inverse hexagonal phase, and the structural characteristics of the observed lamellar phase were affected by varying the lipid acid configuration. In the present study, a transition from a lamellar to an inverse hexagonal phase was detected in the temperature range of approximately 18−22 °C for the MMG-6 analogue (Figure 8). The appearance of a single diffraction peak in the WAXS region at approximately q = 1.5 Å corresponding to a Bragg spacing of d = 4.2 Å suggests that MMG-6 is also in a lamellar gel (L_β) state as mentioned above. Due to the single peak observed, the hydrocarbon chain packing is hexagonal[17] with a chain−chain spacing given by approximately $a_{ch} = 2d/\sqrt{3} \approx 4.9$ Å. This is in agreement with the values for the chain−chain spacings in gel phases reported for other lipids.[17]

Interestingly, the lamellar lattice spacing for MMG-6 of approximately d = 51 Å at 15 °C was notably larger than the lamellar lattice spacing observed for MMG-1 ($d \approx 24$ Å). Furthermore, the additional peak at approximately q = 0.4 $Å^{-1}$, which was observed for both MMG-1, MMG-2 and MMG-3, was not detected for MMG-6. These results indicate that MMG-6 self-assembles into a noninterdigitated L_β phase. As

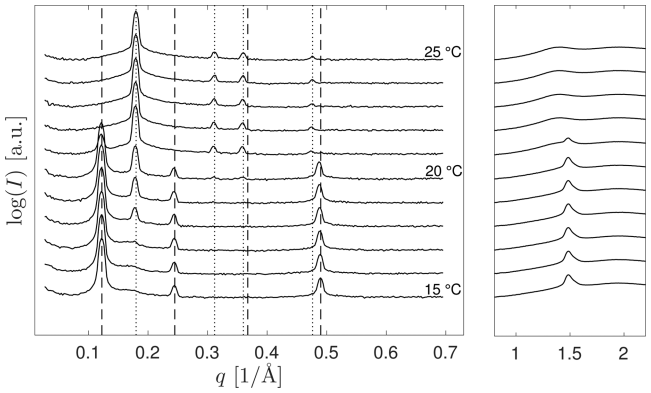

Figure 8. Scattering patterns for MMG-6 in excess buffer in steps of 1 °C in the temperature range of 15−25 °C. A direct transition from a lamellar (dashed lines) to an inverse hexagonal phase (dotted lines) is observed.

expected, a SAXS/WAXS study performed on MMG-7 (differing only in the headgroup stereochemistry), revealed no detectable differences in the self-assembled structures of these mirror image compounds (data not shown). The influence on the structural phase behavior of the lipid acid configuration and the headgroup stereochemistry is summarized in a graphical overview (Figure 9).

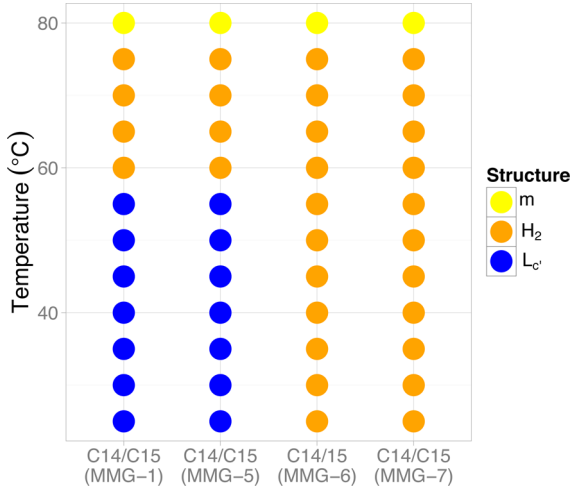

Figure 9. Dependency of the observed structural phases on the stereochemistry of the headgroup and the lipid acid moiety of the MMG analogues in excess buffer. The temperature range is 25−80 °C depicted in steps of 5 °C. MMG-1 from Figure 3 is included for comparison to MMG-5, MMG-6, and MMG-7. Observed structural phases are subgel ($L_{c'}$), inverse hexagonal (H_2), and a complete melting of the lipids (m).

As discussed previously, the propensity of the MMG-6 analogue to form an H_2 phase, in contrast to the $L_{c'}$ phase formed by MMG-1, indicates that the distinct spatial orientation of the hydrocarbon chains of MMG-6 has a pronounced effect on the overall geometrical shape of the molecule.[9] The resulting orientation of the chains allows for a higher degree of positional freedom for the chains, permitting the molecule to adopt a wedge-shaped structure at ambient temperature. A recent similar observation has been made for the major impact of the stereochemistry of the central cyclopentane unit of two synthetic bipolar lipid analogues.[30]

DOI: 10.1021/acs.langmuir.6b01720
Langmuir XXXX, XXX, XXX−XXX

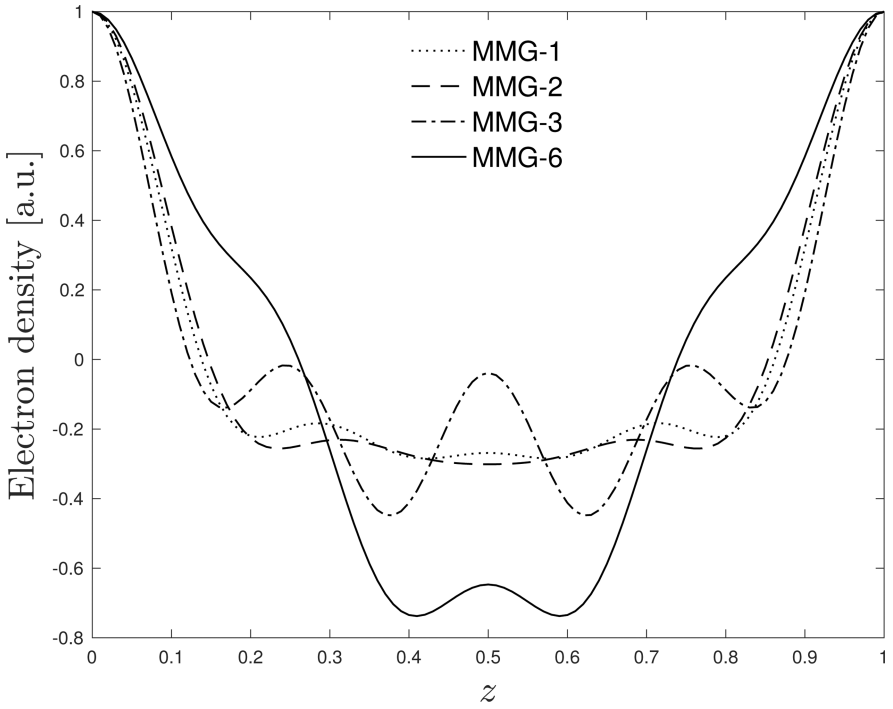

Figure 10. Electron density profiles calculated for MMG-1, MMG-2, MMG-3, and MMG-6. The profiles are normalized to the headgroup peaks and rescaled to a dimensionless unit cell along the bilayer profile axis *z*. The applied fitting parameters are listed in the Supporting Information, Table S1.

Another example is the structural study of the positional isomer of DPPC, *β*-DPPC, which displays a significantly altered phase behavior as compared to DPPC, including among others the formation of an interdigitated bilayer.[31] An additional relevant comparison can be made to a class of synthetic amphiphiles termed gemini surfactants, which are composed of two hydrophilic headgroups with hydrophobic tails linked by a spacer.[32] A recent study revealed that the spacer length, which has a direct influence on the spatial orientation of the hydrophobic tails, has a pronounced effect on the self-assembled structure.[33]

To substantiate the conclusions based on the repeat distance considerations stated above, electron density profiles were calculated following a procedure where false phasing solutions are excluded based on physical arguments[18] (cf. the Supporting Information and Table S1 for further details). For MMG-6, all phasings gave almost identical results. For the other MMG analogues, the constraints were invoked that the headgroup electron density lies at the maximum, and that the structures contain basically no water. Also, profiles with intense positive peaks at the center of the acyl chain domains were ruled out.

Electron density profiles were calculated for MMG-1, MMG-2, MMG-3, and MMG-6 (Figure 10). The electron density profile for the MMG-6 analogue shows the well-known profile of a noninterdigitated bilayer with a minimum at the center of the bilayer.[34,35] The profiles for the analogues MMG-1, MMG-2 and MMG-3, on the other hand, confirm the assignment of interdigitated bilayers for these analogues, since all three profiles show a relatively flat central trough that would be expected for such a chain arrangement, with a higher electron density as compared to the electron density of the non-interdigitated bilayer of MMG-6. All profiles confirm that there is no or little water in the structures because the depicted unit cell is covering the bilayer profile from headgroup to headgroup (Figure 10). Furthermore, the electron density profiles revealed that the headgroups of the analogues with an alternative lipid acid configuration are stronger localized as compared to the headgroups of MMG-6. This is consistent with the interpretation that the headgroups of MMG-1, MMG-2, and MMG-3 are ordered in a 2D lattice, while the headgroups of MMG-6 are not.

It is still not clear why the MMG analogues with an alternative configuration of the lipid acid moiety form interdigitated bilayers, and further studies are needed to fully understand this behavior. Previous studies indicate that a finely tuned balance of interactions between the hydrocarbon chains, the headgroups and the interfacial area is required for the formation of interdigitated bilayers.[36] In the case of DPPC vs *β*-DPPC, it was discussed that the different tilt relative to the glycerol backbone may influence the ability of *β*-DPPC to form interdigitated bilayers as compared to DPPC.[31,36] Thus, in the case of the MMG analogues, the difference in the tilt relative to the hydrophilic headgroup could also result in the formation of interdigitated bilayers for the MMG analogues with an alternative conformation of the lipid acid moiety. In addition, each MMG analogue consists of a mixture of two isomers, which might also affect the packing of the molecules. The formation of enantiomeric segregated lipid gel structures have recently been discussed.[37] However, further studies are needed to elucidate this phenomenon in a more detailed structural investigation.

The relevance of the MMG analogues derives from a subunit vaccine perspective, as they are well-tolerated and display promising immunopotentiating activity.[6,10] A thorough understanding of the nanostructural behavior of these MMG analogues is of importance to enable rational vaccine design because the self-assembling properties of the lipids are key parameters for the nanostructure of particles based on these lipids. Clarifying the nanostructural properties is a prerequisite to enable a controlled tailoring of the vaccine promoting highly

DOI: 10.1021/acs.langmuir.6b01720
Langmuir XXXX, XXX, XXX−XXX

specific immune responses, which is a key aspect for next-generation vaccines.

CONCLUSIONS

In the present study, the effect on the nanostructure due to alterations in the lipid tail length and the stereochemistry of both the headgroup and the lipid acid moiety was elucidated for an array of MMG analogues. All investigated MMG analogues exhibited a direct temperature-induced transition from a lamellar phase to an inverse hexagonal liquid crystalline phase in excess buffer. The study reveals that the MMG analogues with an alternative configuration of the lipid acid moiety (MMG-1, MMG-2, MMG-3, and MMG-5) self-assemble into interdigitated lipid bilayers. Furthermore, this interdigitated lamellar phase was found to be subgel because the lipid headgroups were also in a crystalline state. The two-dimensional superlattice was conserved regardless of the lipid tail lengths.

MMG analogues with a native-like configuration of the lipid acid moiety (MMG-6 and MMG-7), but with the same lipid tail lengths as MMG-1, exhibited a transition from a lamellar phase to an inverse hexagonal phase at a significantly lower temperature as compared to that of MMG-1. Interestingly, these analogues were found to be in an noninterdigitated lamellar gel phase with an observed lattice spacing approximately twice as large as the lamellar lattice spacing measured for MMG-1. The present study also reveals that the configuration of the lipid acid moiety determines whether the MMG analogues adopt an interdigitated or a noninterdigitated lamellar state. Further studies are needed to fully understand why the MMG analogues with an alternative configuration of the lipid acid moiety form interdigitated bilayers.

ASSOCIATED CONTENT

Supporting Information

The Supporting Information is available free of charge on the ACS Publications website at DOI: 10.1021/acs.langmuir.6b01720.

SAXS/WAXS data at the phase transition; SAXS/WAXS data for anhydrous MMG-1; preliminary DSC data for MMG-1; influence of preparation method; electron density calculation details (PDF)

AUTHOR INFORMATION

Corresponding Authors

*E-mail: hxk191@alumni.ku.dk.
*E-mail: jjkk@nbi.dk.
*E-mail: camilla.foged@sund.ku.dk.

ORCID

Anan Yaghmur: 0000-0003-1608-773X
Jacob J. K. Kirkensgaard: 0000-0001-6265-0314

Author Contributions

‖J.J.K.K. and C.F. share senior authorship.

Notes

The authors declare the following competing financial interest(s): This study was partly funded by Statens Serum Institut, a nonprofit government research facility, which holds a patent on the use of MMG in adjuvant formulations.

ACKNOWLEDGMENTS

Thanks to F. Rose, K. J. Vissing (Department of Pharmacy, University of Copenhagen), and J. Nygaard (Niels Bohr Institute, University of Copenhagen) for excellent technical assistance. We kindly acknowledge K. Mortensen (Niels Bohr Institute, University of Copenhagen) for providing the instrument for the SAXS/WAXS studies (funded by the Danish Agency for Science, Technology and Innovation, the Carlsberg Foundation, and Lundbeckfonden), K. Löbmann and T. Rades (Department of Pharmacy, University of Copenhagen) for providing the instrument for the DSC measurements, and D. Christensen (Statens Serum Institut, Denmark) for initial scientific discussions. MAX-lab is acknowledged for providing beamtime and the instrument for a preliminary SAXS study. This work was funded by The Danish Council for Independent Research | Medical Sciences (grant number 09-067412), Statens Serum Institut and The Drug Research Academy (DRA), University of Copenhagen. The Innovation Fund Denmark (Grant Numbers 007-2007-1 and 069-2011-1, and Centre for Nano-Vaccine, Grant Number 09-067052) provided additional funding. The funding sources had no involvement in the study design; in the collection, analysis, or interpretation of data; in the writing of the report; nor in the decision to submit the paper for publication.

REFERENCES

(1) Geisel, R. E.; Sakamoto, K.; Russell, D. G.; Rhoades, E. R. In vivo activity of released cell wall lipids of Mycobacterium bovis Bacillus Calmette-Guérin is due principally to trehalose mycolates. *J. Immunol.* **2005**, *174*, 5007−5015.

(2) Sprott, G. D.; Dicaire, C. J.; Gurnani, K.; Sad, S.; Krishnan, L. Activation of dendritic cells by liposomes prepared from phosphatidylinositol mannosides from Mycobacterium bovis Bacillus Calmette-Guerin and adjuvant activity *in vivo*. *Infect. Immun.* **2004**, *72*, 5235−5246.

(3) Aagaard, C.; Dietrich, J.; Doherty, M.; Andersen, P. TB vaccines: Current status and future perspectives. *Immunol. Cell Biol.* **2009**, *87*, 279−286.

(4) Foged, C. Subunit vaccines of the future: The need for safe, customized and optimized particulate delivery systems. *Ther. Delivery* **2011**, *2*, 1057−1077.

(5) Andersen, C. S.; Agger, E. M.; Rosenkrands, I.; Gomes, J. M.; Bhowruth, V.; Gibson, K. J.; Petersen, R. V.; Minnikin, D. E.; Besra, G. S.; Andersen, P. A simple mycobacterial monomycolated glycerol lipid has potent immunostimulatory activity. *J. Immunol.* **2009**, *182*, 424−432.

(6) Nordly, P.; Korsholm, K. S.; Pedersen, E. A.; Khilji, T. S.; Franzyk, H.; Jorgensen, L.; Nielsen, H. M.; Agger, E. M.; Foged, C. Incorporation of a synthetic mycobacterial monomycoloyl glycerol analogue stabilizes dimethyldioctadecylammonium liposomes and potentiates their adjuvant effect *in vivo*. *Eur. J. Pharm. Biopharm.* **2011**, *77*, 89−98.

(7) Tritto, E.; Mosca, F.; De Gregorio, E. Mechanism of action of licensed vaccine adjuvants. *Vaccine* **2009**, *27*, 3331−3334.

(8) Delany, I.; Rappuoli, R.; De Gregorio, E. Vaccines for the 21st century. *EMBO Mol. Med.* **2014**, *6*, 708−720.

(9) Martin-Bertelsen, B.; Korsholm, K. S.; Rose, F.; Nordly, P.; Franzyk, H.; Andersen, P.; Agger, E. M.; Christensen, D.; Yaghmur, A.; Foged, C. The supramolecular structure is decisive for the immunostimulatory properties of synthetic analogues of a mycobacterial lipid *in vitro*. *RSC Adv.* **2013**, *3*, 20673−20683.

(10) Martin-Bertelsen, B.; Korsholm, K. S.; Roces, C. B.; Nielsen, M. H.; Christensen, D.; Franzyk, H.; Yaghmur, A.; Foged, C. Nano-Self-Assemblies Based on Synthetic Analogues of Mycobacterial Monomycoloyl Glycerol and DDA: Supramolecular Structure and Adjuvant Efficacy. *Mol. Pharmaceutics* **2016**, *13*, 2771−2781.

DOI: 10.1021/acs.langmuir.6b01720
Langmuir XXXX, XXX, XXX−XXX

(11) Hyde, S.; Blum, Z.; Landh, T.; Lidin, S.; Ninham, B. W.; Andersson, S.; Larsson, K. *The Language of Shape. The Role of Curvature in Condensed Matter: Physics, Chemistry and Biology*, 1st ed.; Elsevier Science B.V.: Amsterdam, 1996.
(12) Nagle, J. F.; Tristram-Nagle, S. Structure of lipid bilayers. *Biochim. Biophys. Acta, Rev. Biomembr.* **2000**, *1469*, 159−195.
(13) Shearman, G. C.; Ces, O.; Templer, R. H.; Seddon, J. M. Inverse lyotropic phases of lipids and membrane curvature. *J. Phys.: Condens. Matter* **2006**, *18*, 1105.
(14) Fong, C.; Le, T.; Drummond, C. J. Lyotropic liquid crystal engineering-ordered nanostructured small molecule amphiphile self-assembly materials by design. *Chem. Soc. Rev.* **2012**, *41*, 1297−1322.
(15) Huang, T. C.; Toraya, H.; Blanton, T. N.; Wu, Y. X-ray powder diffraction analysis of silver behenate, a possible low-angle diffraction standard. *J. Appl. Crystallogr.* **1993**, *26*, 180−184.
(16) Rappolt, M. *Advances in Planar Lipid Bilayers and Liposomes*; Elsevier: Amsterdam, 2006; Vol. *5*, Chapter 9, pp 253−283.
(17) Marsh, D. Lateral order in gel, subgel and crystalline phases of lipid membranes: Wide-angle X-ray scattering. *Chem. Phys. Lipids* **2012**, *165*, 59−76.
(18) Bottier, C.; Géan, J.; Artzner, F.; Desbat, B.; Pézolet, M.; Renault, A.; Marion, D.; Vié, V. Galactosyl headgroup interactions control the molecular packing of wheat lipids in Langmuir films and in hydrated liquid-crystalline mesophases. *Biochim. Biophys. Acta, Biomembr.* **2007**, *1768*, 1526−1540.
(19) Marsh, D. *Handbook of Lipid Bilayers*, 2nd ed.; CRC Press: Boca Raton, FL, 2013.
(20) Tyler, A.; Law, R.; Seddon, J. M. In *Methods In Membrane Lipids*; Owen, D., Ed.; Springer: New York, 2015; Vol. *1232*, Chapter 16.
(21) Lewis, R. N. Studies of the Thermotropic Phase Behavior of Phosphatidylcholines Containing 2-Alkyl Substituted Fatty Acyl Chains: A New Class of Phosphatidylcholines Forming Inverted Nonlamellar Phases. *Biophys. J.* **1994**, *66*, 1088−1103.
(22) Katsaras, J.; Raghunathan, V. A.; Dufourc, E. J.; Dufourcq, J. Evidence for a Two-Dimensional Molecular Lattice in Subgel Phase DPPC Bilayers. *Biochemistry* **1995**, *34*, 4684−4688.
(23) Katsaras, J. Structure of the subgel ($L_{c'}$) and gel ($L_{\beta'}$) phases of oriented dipalmitoylphosphatidylcholine multibilayers. *J. Phys. Chem.* **1995**, *99*, 4141−4147.
(24) Raghunathan, V. A.; Katsaras, J. Structure of the $L_{c'}$ phase in a hydrated lipid multilamellar system. *Phys. Rev. Lett.* **1995**, *74*, 4456−4459.
(25) Takahashi, H.; Hatta, K.; Hatta, I. Growth of Molecular Superlattice in Fully Hydrated Dipalmitoylphosphatidylcholine during Subgel Phase Formation Process. *J. Phys. II* **1996**, *6*, 1657−1662.
(26) Koynova, R.; Tenchov, B. Transitions between lamellar and non-lamellar phases in membrane lipids and their physiological roles. *OA Biochemistry* **2013**, *1*, 1−9.
(27) Mannock, D. A.; Lewis, R. N.; McElhaney, R. N. Physical properties of glycosyl diacylglycerols. 1. Calorimetric studies of a homologous series of 1,2-di-O-acyl-3-O-(α-D-glucopyranosyl)-sn-glycerols. *Biochemistry* **1990**, *29*, 7790−7799.
(28) Sen, A.; Hui, S. W.; Mannock, D. A.; Lewis, R. N.; McElhaney, R. N. Physical Properties of Glycosyl Diacylglycerols. 2. X-Ray Diffraction Studies of a Homologous Series of 1,2-Di-O-acyl-3-O-(α-D-Glucopyranosyl)-sn-Glycerols. *Biochemistry* **1990**, *29*, 7799−7804.
(29) Koynova, R.; MacDonald, R. C. Cationic O-ethylphosphatidylcholines and their lipoplexes: phase behavior aspects, structural organization and morphology. *Biochim. Biophys. Acta, Biomembr.* **2003**, *1613*, 39−48.
(30) Jacquemet, A.; Mériadec, C.; Lemiègre, L.; Artzner, F.; Benvegnu, T. Stereochemical effect revealed in self-assemblies based on archaeal lipid analogues bearing a central five-membered carbocycle: a SAXS study. *Langmuir* **2012**, *28*, 7591−7597.
(31) Serrallach, E. N.; Dijkman, R.; de Haas, G. H.; Shipley, G. G. Structure and thermotropic properties of 1,3-dipalmitoyl-glycero-2-phosphocholine. *J. Mol. Biol.* **1983**, *170*, 155−174.
(32) Menger, F. M.; Littau, C. A. Gemini surfactants: A new class of self-assembling molecules. *J. Am. Chem. Soc.* **1993**, *115*, 10083−10090.
(33) Sorenson, G. P.; Coppage, K. L.; Mahanthappa, M. K. Unusually Stable Aqueous Lyotropic Gyroid Phases from Gemini Dicarboxylate Surfactants. *J. Am. Chem. Soc.* **2011**, *133*, 14928−14931.
(34) Harper, P. E.; Mannock, D. A.; Lewis, R. N.; McElhaney, R. N.; Gruner, S. M. X-ray diffraction structures of some phosphatidylethanolamine lamellar and inverted hexagonal phases. *Biophys. J.* **2001**, *81*, 2693−2706.
(35) Heberle, F. A.; Pan, J.; Standaert, R. F.; Drazba, P.; Kučerka, N.; Katsaras, J. Model-based approaches for the determination of lipid bilayer structure from small-angle neutron and X-ray scattering data. *Eur. Biophys. J.* **2012**, *41*, 875−890.
(36) Smith, E. A.; Dea, P. K. In *Applications of Calorimetry in a Wide Context - Differential Scanning Calorimetry, Isothermal Titration Calorimetry and Microcalorimetry*; Elkordy, A. A., Ed.; InTech: Rijeka, Croatia, 2013; Chapter 18.
(37) Horta, B. A. C.; Hünenberger, P. H. Enantiomeric segregation in the gel phase of lipid bilayers. *J. Am. Chem. Soc.* **2011**, *133*, 8464−8466.

DOI: 10.1021/acs.langmuir.6b01720
Langmuir XXXX, XXX, XXX−XXX